



# Foxtail millet bran-derived phenolic acids ameliorate insulin resistance by non-competitively inhibiting $\alpha$ -glucosidase activity and blocking miR-1-3p/PTP1B signaling axis in diabetic mice

Jiangying Shi <sup>a,1</sup>, Jin Wang <sup>a,1</sup>, Shuhua Shan <sup>a</sup>, Mengyun Zhao <sup>a</sup>, Cai Bi <sup>a</sup>, Hanqing Li <sup>b,\*</sup>, Zhuoyu Li <sup>a,\*</sup>

<sup>a</sup> Institute of Biotechnology, Key Laboratory of Chemical Biology and Molecular Engineering of National Ministry of Education, Shanxi University, Taiyuan, China  
<sup>b</sup> College of Life Science, Shanxi University, Taiyuan 030006, China



## ARTICLE INFO

### Keywords:

Foxtail millet bran  
 Phenolic acids  
 miRNA  
 PTP1B  
 Insulin resistance

## ABSTRACT

As the prevalence of type 2 diabetes continues to rise, traditional treatment has not been effectively controlled. Therefore, it is urgent to explore safe and effective hypoglycemic substances. In our previous studies, phenolic acids extracted from foxtail millet bran (BPIS) could inhibit cancer cells proliferation by inhibiting glucose uptake, suggesting that BPIS may play a role in regulating glucose metabolism. However, the role of BPIS in improving diabetes remains unclear. The results of this study revealed that the antidiabetic activity of BPIS was characterized by non-competitive inhibition of  $\alpha$ -glucosidase activity, blocking the gluconeogenic rate-limiting enzyme phosphoenolpyruvate carboxylase (PEPCK) and the expression of the negative regulator of insulin signaling, protein tyrosine phosphatase (PTP1B). In addition, this study further revealed that BPIS can improve insulin resistance by upregulating miR-1-3p and inhibiting expression of its target gene PTP1B, which proves that BPIS is an important functional component of the anti-diabetic potential of bran.

## 1. Introduction

Type 2 diabetes mellitus (T2DM) is a chronic metabolic disease that is the main cause of many complications such as cardiovascular disease, diabetic nephropathy and diabetic foot, and its prevalence is gradually increasing worldwide, which has become an urgent public health problem(Lebovitz, 2001; Ruze et al., 2023; Xu, Li, Dai, & Peng, 2018). Insulin resistance is one of the important characteristics of T2DM, and improving insulin sensitivity is of great significance for the treatment of T2DM(Lebovitz, 2001). Although current clinical drugs for the treatment of diabetes can effectively improve insulin resistance, their treatment cycle is long and they are often accompanied by side effects such as edema, liver damage, obesity, and damage to the stomach and intestines (Wu, Liu, Jiang, & Fang, 2020). Therefore, screening active molecules that can safely and effectively improve insulin sensitivity has become a promising strategy for T2DM treatment.

Foxtail millet (*Setaria italica*) is an annual grass plant, the main crop grown in northern China(Samtiya, Aluko, Dhaka, Dhewa, & Punya, 2023). It is a good source of polyphenols, proteins, dietary fiber, and trace elements(Chandrasekara & Shahidi, 2010). Previous studies have found that millet bran phenolic acids prevent atherosclerosis by remodeling the gut microbiota (Liu et al., 2021). A novel peroxidase extracted from foxtail millet bran displayed anti-colorectal cancer(Shan et al., 2015). Foxtail millet lipid extract can improve the symptoms of diabetic mice(H. Wang et al., 2023). Furthermore, Sireesha et al. (Sireesha, Kasetti, Nabi, Swapna, & Apparao, 2011) have reported that millet aqueous extract could significantly reduce the fasting blood glucose value of rats. The bran shed during the processing of millet is rich in polyphenols (Chandrasekara & Shahidi, 2011). However, there are few reports on the improvement of diabetes by polyphenols extracted from foxtail millet.

PTP1B is an important regulator of insulin signaling that negatively

**Abbreviations:** BPIS, bound phenolic acids of inner shell; PEPCK, phosphoenolpyruvate carboxylase; PTP1B, protein tyrosine phosphatase; IRb, insulin receptor b subunit; IRS-2, insulin receptor substrate-2; Met, metformin; STZ, streptozotocin; GLUT2, glucose transporter 2; OGTT, oral glucose tolerance test; T2DM, type 2 diabetes mellitus..

\* Corresponding authors.

E-mail addresses: [13903461328@139.com](mailto:13903461328@139.com) (H. Li), [lzy@sxu.edu.cn](mailto:lzy@sxu.edu.cn) (Z. Li).

<sup>1</sup> These authors contributed equally to this work.

<https://doi.org/10.1016/j.jff.2024.106105>

Received 24 November 2023; Received in revised form 28 January 2024; Accepted 27 February 2024

Available online 3 March 2024

1756-4646/© 2024 The Authors. Published by Elsevier Ltd. This is an open access article under the CC BY-NC-ND license (<http://creativecommons.org/licenses/by-nd/4.0/>).

regulates insulin signal transduction through catalytic activation of the N-terminal of insulin receptor and dephosphorylation of tyrosine residues of insulin receptor substrate (Z. Y. Zhang & Lee, 2003). It has been reported that anthocyanins in blueberry, mulberry, cranberry and cranberry can reduce blood glucose by inhibiting PTP1B (Xiao, Guo, Sun, & Zhao, 2017). Gonzalez-rodriguez et al. (González-Rodríguez et al., 2010) found that resveratrol can reduce the expression of PTP1B in insulin receptor substrate 2 (IRS2) deficient mice and STZ-induced mice, thereby enhancing the insulin sensitivity of mice. MicroRNAs (miRNAs) are endogenous small non-coding RNAs nearly 21 bases in length, which regulate the expression of target proteins by regulating the expression level of genes after transcription (X. Wang, He, Mackowiak, & Gao, 2021). MiRNAs play an important role in glucose metabolism and insulin signal, potentially affecting glucose homeostasis and the development of diabetes (Ali et al., 2023). Ding et al. (X. Q. Ding et al., 2015) found that curcumin can improve insulin signal transduction by activating the expression of miR-206 and down-regulating PTP1B, thereby protecting the body from fructose-induced damage of renal podocyte. Yang et al. (Yang, Seo, Kim, & Kim, 2012) study showed that flavonoids from glycyrrhizae could improve insulin resistance by promoting miRNA-122 and inhibiting PTP1B expression, suggesting that miRNA could participate in the improvement of plant polyphenols on diabetes.

In our previous studies, phenolic acids extracted from foxtail millet bran (BPIS) could inhibit proliferation of colon cancer cells by inhibiting glucose uptake, suggesting that BPIS may play a role in regulating glucose metabolism. BPIS was mainly phenolic acids by LC-MS/MS identification, including ferulic acid, p-coumaric acid, 4-O- $\beta$ -D-pyranoside vanillic acid, Glucosyl syringic acid, ferulic acid 4-O- $\beta$ -D-pyranoside, 4-hydroxybenzoic acid, vanillic acid, syringic acid, isoferulic acid, dimeric ferulic acid derivatives, vitexin and dimeric cinnamic acid derivatives (Lu et al., 2018). Therefore, the highlight of this study is to determine the key role of miRNA in BPIS to improve insulin sensitivity. In this study, the enzyme-inhibitor model experiment was firstly used to confirm that BPIS significantly inhibited the activity of polysaccharide hydrolase ( $\alpha$ -glucosidase), and the inhibition category was non-competitive. Secondly, BPIS improved glucose metabolism disorder by inhibiting PTP1B in insulin-resistant HepG2 cell model. Subsequently, it was found that the expression level of PTP1B in cells was negatively correlated with miRNA-1-3p. PTP1B was confirmed to be the target gene of miRNA-1-3p by software prediction combined with double luciferase reporter vector experiment. The role of miRNA-1-3p/PTP1B signal axis in mediating BPIS to improve glucose metabolism disorder is further clarified in insulin-resistant HepG2 cell model and diabetic mouse model. These results provided effective experimental and theoretical basis for the development of insulin sensitizer and nutritional intervention of phenolic acids derived from foxtail millet bran.

## 2. Materials and methods

### 2.1. Reagents and antibodies

RPMI-1640 (v/v = 1:1) medium and fetal bovine serum (FBS) were purchased from GIBCO (Grand Island, NY, USA). Glucose Test Kit was obtained from Biovision (California, USA). The BCA protein kit was purchased from Thermo Fisher (Shanghai, China). RNAiso Plus, Prime-Script RT Master Mix and SYBR Green PCR Master Mix were obtained from TAKARA (Shiga, Japan); Antibodies against PEPCK and PTP1B were purchased from Cell Signaling Technology Company (Shanghai, China). Antibody for GAPDH and PCNA were from Abmart (Arlington, MA, USA). Penicillin and streptomycin were purchased from GIBCO (Thermo Fisher Scientific, Waltham, MA, USA). Oligonucleotide primers were synthesized by GenePharm (Shanghai, China). SYBR Premix Ex Taq were purchased from TAKARA (Dalian, China). Puromycin and polybrene were purchased from Sigma-Aldrich (St. Louis, MO, USA).

### 2.2. Cell culture and cell model of insulin resistance

Human hepatoma HepG2 cell line was purchased from the Cell Bank of Type Culture Collection of The Chinese Academy of Sciences (CAS, Shanghai, China). Cells were grown in RPMI-1640 medium supplemented with 10 % (v/v) heat-inactivated fetal calf serum, 2 mmol/L glutamine, 100 units/ml penicillin, and 100 mg/mL streptomycin (Sigma; St. Louis, MO, USA) at 37 °C in a 5 % CO<sub>2</sub> humidified atmosphere. To construct a cell model of insulin resistance, digested HepG2 cells were inoculated into 96-well plate with 10<sup>4</sup> cells per well. When the density of adherent cells reaches 90 %, the concentration of 10<sup>-8</sup> mol/L insulin is added to the 96 well plate and cultured in an incubator for 36 h. The medium containing serum was replaced with serum free medium and continue to incubate for 12 h to collect the medium. Glucose content was measured using a glucose oxidase assay kit to analyze the degree of insulin resistance of HepG2 cells.

### 2.3. $\alpha$ -glucosidase inhibition assay

Acetone powder from rat intestine (Sigma Chem Co. Ltd., product I1360) was extracted as a source of  $\alpha$ -glucosidase. The determination of  $\alpha$ -glucosidase activity was slightly modified from (McDougall et al., 2005). The final concentrations of BPIS and  $\alpha$ -glucosidase were 50, 100, 150  $\mu$ g/mL and 40  $\mu$ L (1.33 mg  $\alpha$ -glucosidase), respectively. After incubation at 37 °C for 10 min, 120  $\mu$ L (1  $\mu$ g/ $\mu$ L) maltose was added, and after incubation at 37 °C for 30, 60 and 90 min, 50  $\mu$ L 1 mol/L Tris-HCl was added to terminate the reaction. The measurement was conducted using the glucose oxidase assay kit (APPLYGEN, Beijing, China).

### 2.4. $\alpha$ -glucosidase inhibition type assay

BPIS with final concentrations of 0, 50, 150  $\mu$ g/mL and  $\alpha$ -glucosidase were added and incubated at 37 °C for 10 min. After that, 120  $\mu$ L maltose with final concentrations of 14, 21, 28, 35, 56 mM was added and incubated at 37 °C for 20 min. The reaction was terminated by 1 mol/L Tris-HCl. Taking 1/V as the ordinate and 1/S as the abscissa, the Lineweaver-Burk double reciprocal curve was made. The intersection point of the line with the horizontal axis was  $-1/K_m$ , and the intersection point of the line with the vertical axis was  $1/V_{max}$ . Where 1/V is the initial velocity of the reaction at this substrate concentration, 1/S is the inverse of the substrate concentration, and 1/K<sub>m</sub> is the inverse of Michaelis constant.

### 2.5. Isolation of total RNA and real-time polymerase chain reaction

Total RNA from human hepatoma cells was prepared using TRIzol (Takara, Dalian, China) and 500 ng of RNA was reverse transcribed to cDNA using PrimeScript II first Strand cDNA Synthesis Kit (Takara, Dalian, China). Quantitative PCR was performed using SYBR Premix Ex TaqII (Takara) on a bio-rad real-time PCR system. The quantitative PCR primers used were as follows: 1) PEPCK 5' -CAGGCTG GAAAGTG-GAGTGTGTG-3' (Forward); 5' -TGGGATTGGTGGCAGAGG-3' (Reverse); 2) PTP1B 5' -TCAAAGTCCGAGAGTCAGGGTCAC -3' (Forward); 5' -CATCAGCAAGAGGCAGGTATCAGC -3' (Reverse). The miRNA expression level was measured by real-time polymerase chain reaction (PCR) with a SYBR Premix Ex Taq (TAKARA, Dalian, China). U6 was used as the control. Gene expression was quantified according to the 2<sup>-ΔΔCt</sup> method.

### 2.6. DNA construct, MiRNA mimic and inhibitor transfection

PTP1B was subcloned into the pLVX-AcGFP3-N1 (GFP) vector to generate the GFP-PTP1B vector. To overexpression PTP1B, HepG2 cells were transfected GFP-PTP1B plasmid. The Transfection of GFP or GFP-PTP1B vectors was performed using Turbofect (Thermo Scientific, MA, USA) according to the manufacturer's instructions.

HepG2 cells were inoculated into six-well plates and the miRNA mimics and inhibitors (GenePharma, Shanghai, China) were transfected using the HiPerFect transfection reagent (QIAGEN, Shanghai, China) when the density of adherent cells reaches 80 %. The oligonucleotides and the HiperFect Transfection Reagent were added into serum-free medium, mixed homogeneously, kept at room temperature for 15 min, then gently drip into a six-well plate for rapid mixing. The medium containing the transfection reagent was replaced with fresh media after transfecting for 6 h. The transfection efficiency was analyzed by quantitative PCR (qPCR).

### 2.7. Dual-luciferase assay

The PTP1B 3'-UTR was subcloned into the psicheck-2 vector (Promega, Madison, WI) to generate the psicheck2-PTP1B-3'UTR vector. HepG2 cells were cotransfected with psicheck2-PTP1B-3'UTR or control (psicheck2) vectors and either 50 nM of the miR-1-3p or negative control (NC mimic) mimics, or miR-1-3p or negative control (NC inhibitor) inhibitors using the HiPerFect transfection reagent. At 48 h post-transfection, cells were lysed and the luciferase activity was measured according to the manufacturer's instructions. The results were normalized to the activity of the renilla luciferase gene.

### 2.8. Western blotting

Total protein was extracted from cells using RIPA lysis buffer. The BCA protein assay was performed to measure total protein concentrations. Cell lysates (60 mg) were added to 10 % SDS-PAGE for separation and transferred to polyvinylidene fluoride (PVDF) membranes. A blocking solution (5 % fresh milk in TBS plus Tween 20) was used to block nonspecific binding to PVDF membranes at room temperature for 1 h. PVDF membranes were incubated with the primary antibody overnight at 4°C and with secondary antibodies for 2 h at room temperature. Signals were recorded using an enhanced chemiluminescence detection kit and a radiographic film (CARESTREAM; 5 in.\*7 in.).

### 2.9. Animal studies

Forty-five male ICR mice (four-week-old) obtained from the Beijing changyang xishan farm (Beijing, China), were housed and maintained under laboratory conditions of temperature of 18–22 °C, relative humidity of 40–60 %, with a 12 h light and 12 h dark cycles. All protocols for animal experiments were accepted by the Institutional Animal Care and Use Committee of the Laboratory Animal Center, Shanxi Provincial People's Hospital. Mice were provided with ultraviolet radiation sterilized diets, autoclaved water, and autoclaved bedding was replaced weekly. After acclimation for 1 week, mice were randomly divided into four groups: 1) control group, 2) model group, 3) Metformin group and 4) BPIS group. The control group was kept on the ordinary diet, and the diets of the other groups were changed to high-sugar and high-fat diet. Diabetes was induced by an intraperitoneal injection with either 50 mg/kg streptozotocin (STZ) (dissolved in Citrate - sodium citrate buffer) for four consecutive days. The control group was injected with the same volume of citrate and sodium citrate buffer. Mice were subjected to tail tip blood sampling, and blood glucose levels were measured using a glucometer (ARKRAY(GT1970), Shanghai, China). After STZ injection, mice were fasted for 12 h, and fasting blood glucose was measured, the mice with blood glucose level greater than 11.1 mmol/L were selected as the successful model. After the successful establishment of diabetic mouse model, the experimental group continued to be fed with high-sugar and high-fat diet, while the control group continued to be fed with ordinary diet until the end of the experiment. The positive control group was given 150 mg/kg metformin solution, and the BPIS group was given 100 mg/kg BPIS solution. After 4 weeks of metformin and BPIS administration, all mice were fasted for 12 h, anesthetized with ether, and blood was collected from eyeballs and stored in a refrigerator at

-80°C. All the mice were sacrificed by cervical dislocation, and the liver and pancreas were collected and stored in liquid nitrogen.

### 2.10. Histopathology and immunohistochemistry assays

The liver and pancreas were fixed with 4 % buffered formalin and embedded in paraffin. Next, these fixed organs were stained using hematoxylin and eosin (H&E) to observe histological features. For IHC staining, the paraffin sections were dewaxed in xylene and dehydrated in concentration gradient ethanol. After an antigen retrieval process and blocking. Antigen retrieval was carried out using citrate buffer (pH 6.0). All sections were stained with primary antibodies against PTP1B and GLUT-2. Subsequently, these stained sections were visualized and photographed under an inverted microscope (100× magnification). IHC data were quantified using Image J software.

### 2.11. Oral glucose tolerance test (OGTT)

After 12 h of fasting, mice were given a glucose solution by gavage (1 g/kg). Thereafter, we used a One Touch Glucose Meter (Johnson & Johnson, NH, USA), from a tail prick, to determine blood glucose levels at 0, 30, 60, 90, and 120 min and calculated the area under the time-blood glucose curve to represent the magnitude of glucose response.

### 2.12. Determinations of insulin and glycated serum protein in serum

The levels of insulin and glycosylated serum protein in mouse serum were determined according to the instructions of ELISA kit (Meimian, Jiangsu, China).

### 2.13. Statistical analysis

Data were presented as means  $\pm$  standard deviation (SD) calculated over three independent experiments performed in triplicate. Origin Pro 8 software was used to create the artwork. The comparisons between two groups were analyzed by Student's *t*-test or Multiple comparisons were analyzed by one-way factorial analysis of variance (ANOVA). \**p* < 0.05 is indicated significant differences between two groups. \*\**p* < 0.01 is considered highly significant differences between two groups.

## 3. Results

### 3.1. BPIS inhibits $\alpha$ -glucosidase activity *in vitro*

To evaluate the hypoglycemic activity of BPIS, enzymes-inhibitor model was used to examine the inhibition effects of BPIS at various concentrations (50  $\mu$ g/mL, 100  $\mu$ g/mL and 150  $\mu$ g/mL) and different action times (30 min, 60 min, 90 min) for  $\alpha$ -glucosidase activity. The results showed that when the reaction time was 60 min, the inhibition rate of 150  $\mu$ g/mL BPIS on  $\alpha$ -glucosidase activity reached  $58.68 \pm 0.88$  %. When the reaction time was 90 min, the inhibition rate of 100  $\mu$ g/mL and 150  $\mu$ g/mL BPIS on  $\alpha$ -glucosidase activity reached 60.63 % and 64.23 %, respectively (Fig. 1A). These results indicate that BPIS has a significant inhibitory effect on  $\alpha$ -glucosidase activity in a time-dependent and dose-dependent manner. To determine the type of inhibition of  $\alpha$ -glucosidase by BPIS, a Lineweaver-Burk double-reciprocal curve was drawn, showing all straight lines intersect on the horizontal axis, that is, as the concentration of BPIS increases, the value of *K<sub>m</sub>* does not change and the value of *V<sub>max</sub>* decreases (Fig. 1B, C). These results suggest that the type of inhibition of  $\alpha$ -glucosidase activity by BPIS was noncompetitive combination.

### 3.2. Hepatocellular carcinoma cells are constructed to model insulin resistance

Insulin resistance is the decrease in the sensitivity of tissues and

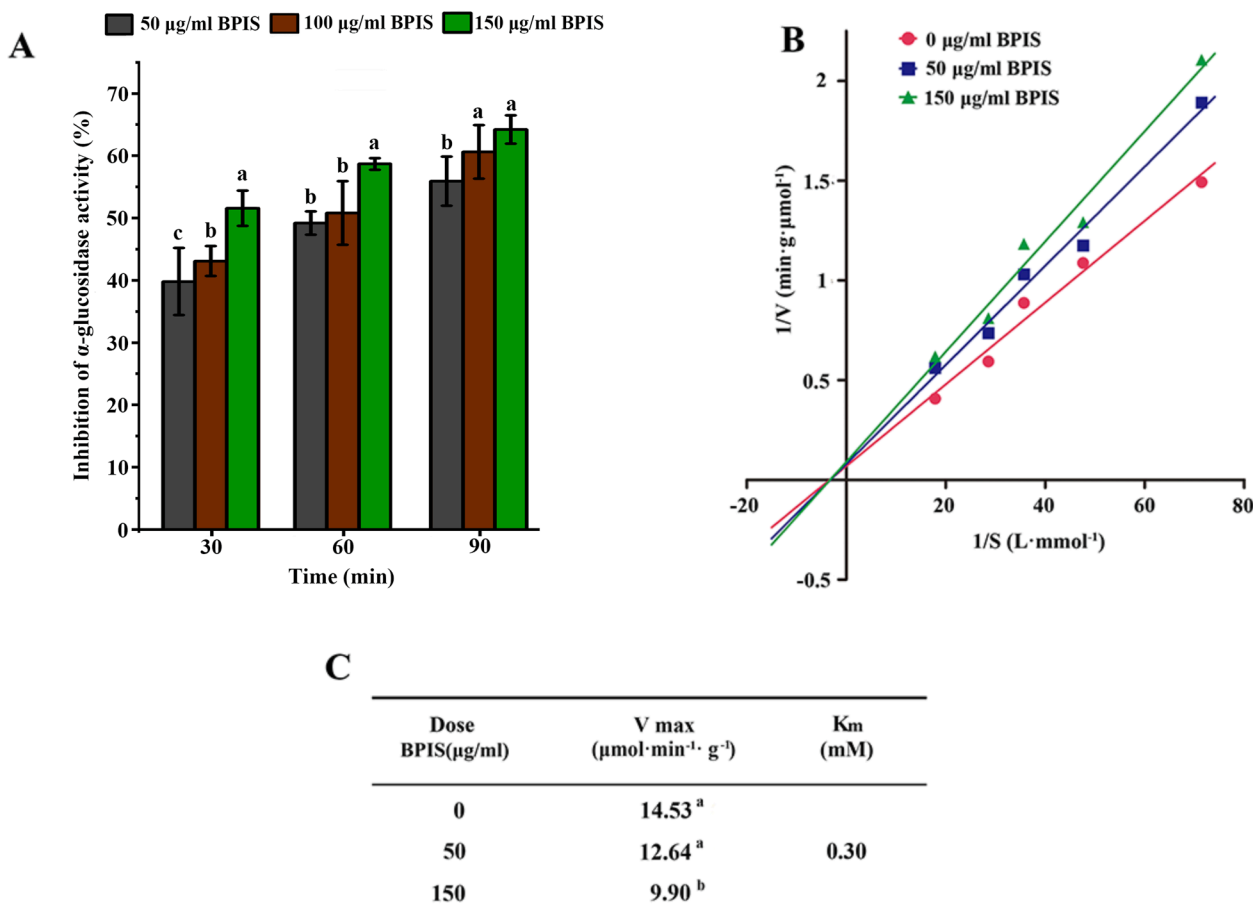


**Fig. 1.** Effects of BPIS on inhibitory of  $\alpha$ -glucosidase activity. (A) The inhibition rate of  $\alpha$ -glucosidase activity was calculated by measuring the absorbance treated with different concentrations of BPIS (50, 100, 150 µg/mL) for different time (30, 60, 90 min). Significant differences in the group were indicates by different letters,  $*p < 0.05$ . (B) At different substrate concentrations (14, 21, 28, 35, 56 mM), the enzyme kinetics curves treated with different concentrations of BPIS (0, 50, 150 µg/mL) were plotted. (C) Effects of BPIS on the kinetic constants of  $\alpha$ -glucosidase.

organs to insulin, resulting in a decrease in glucose consumption (Groop, 2000). Therefore, the decrease in glucose consumption is used as the construction criterion for diabetic model. HepG2 cells are ideal cells to study the pathogenesis of insulin resistance and the action mechanism of hypoglycemic substances (Gurnell, Savage, Chatterjee, & O'Rahilly,

2003). In this study, HepG2 cells were induced by hyper-insulin to establish insulin resistance model to evaluate the hypoglycemic effect of BPIS. At the insulin concentration of  $10^{-8}$  mol/L, the consumption of glucose by HepG2 cells was significantly decrease from that of the normal control (Fig. 2A). Hence,  $10^{-8}$  mol/L was selected as the optimal

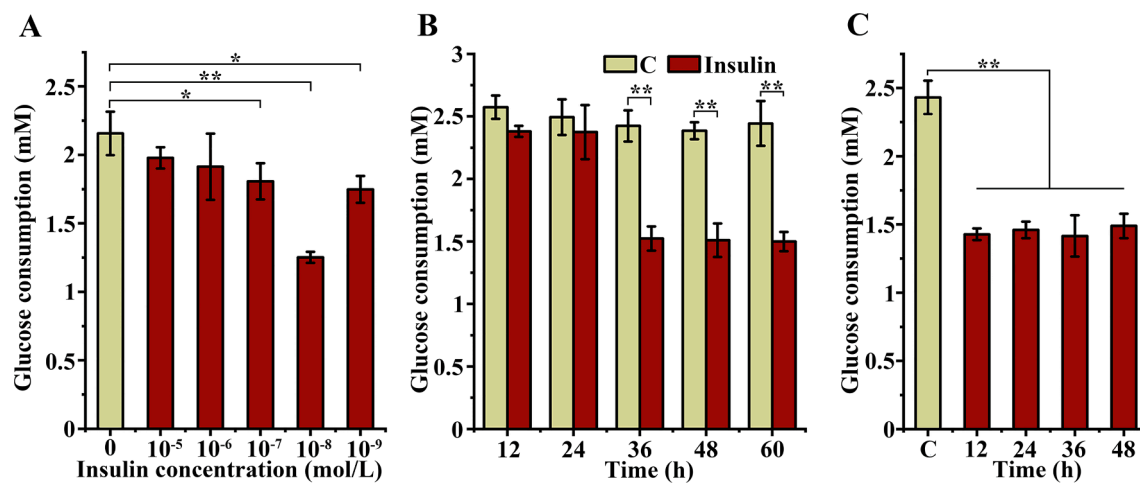


**Fig. 2.** Establishment of insulin resistance cell model. (A) Glucose consumption was measured when HepG2 cells were treated with different concentrations of insulin ( $10^{-5}$ ,  $10^{-6}$ ,  $10^{-7}$ ,  $10^{-8}$ ,  $10^{-9}$  mol/L) for 36 h. (B) Glucose consumption was measured when HepG2 cells were treated with  $10^{-8}$  mol/L insulin for different time (12, 24, 36, 48, 60 h). (C) HepG2 cells were treated with  $10^{-8}$  mol/L insulin for 36 h, and then glucose consumption was measured when cultured in fresh medium for different time (12, 24, 36 and 48 h).  $*p < 0.05$ ,  $**p < 0.01$ ,  $n = 3$ .

concentration for establishing insulin resistance model. As shown in Fig. 2B, glucose consumption was significantly decrease after treating cells with  $10^{-8}$  mol/L insulin for 36 h. Therefore, it was determined that  $10^{-8}$  mol/L of insulin induced cells for 36 h as the optimal condition for constructing the insulin resistance HepG2 cell model. Further, to determine the stability of the insulin resistance model. Model and control cells were incubated in insulin-free medium and glucose consumption was measured at 12, 24, 36 and 48 h, respectively. As shown in Fig. 2C, cell glucose consumption decreased significantly after 12 h and continued to 48 h. These results indicate that the HepG2 cell model of insulin resistance has been successfully constructed *in vitro*.

### 3.3. BPIS improves the insulin resistance of HepG2 cells

To determine the ameliorative effect of BPIS on glucose metabolism disorder, we treated insulin-resistant HepG2 cells with different concentrations of BPIS. As shown in Fig. 3A, glucose consumption was significantly decreased in the model group compared with the normal control group, but it gradually recovered and tended to be normal by BPIS treatment. It has been shown that phosphoenolpyruvate carboxylase (PEPCK) is a rate-limiting enzyme in gluconeogenesis and protein tyrosine phosphatase (PTP1B) is a negative regulator of insulin signaling (Cadoudal, Fouque, Benelli, & Forest, 2008; Goldstein, 2001). Therefore, we examined changes in the mRNA and protein levels of PEPCK

and PTP1B in BPIS-treated insulin-resistant HepG2 cell models. The results showed that the expression levels of PEPCK and PTP1B were significantly up-regulated in the insulin resistance cell model at both RNA level (Fig. 3B-C) and protein level (Fig. 3D-E). However, BPIS treatment significantly reversed PEPCK and PTP1B expression in a concentration dependent manner (Fig. 3B-E). These results indicate that BPIS could improve insulin resistance by inhibiting the expression of PEPCK and PTP1B.

### 3.4. BPIS improves glucose metabolism disorders by inhibiting PTP1B

Overexpression of PTP1B catalyzes dephosphorylation of tyrosine residues of insulin receptor  $\beta$  subunit (IR $\beta$ ) and insulin receptor substrate-2 (IRS-2), thereby promoting insulin resistance. Therefore, inhibition of PTP1B expression has become an effective strategy for the treatment of diabetes. We next determined whether PTP1B plays a key role in the improvement of insulin resistance by BPIS. We constructed GFP-PTP1B plasmid to transfet HepG2 cells and observed the transfection efficiency by fluorescence inverted microscope. As shown in Fig. S4A-B, cells with green fluorescence after transfection were observed under a fluorescence microscope, which preliminarily indicated that the transfection was successful. qPCR and western blot were used to detect the transfection efficiency. At the RNA level, the expression of PTP1B in cells transiently transfected with GFP-PTP1B was up-

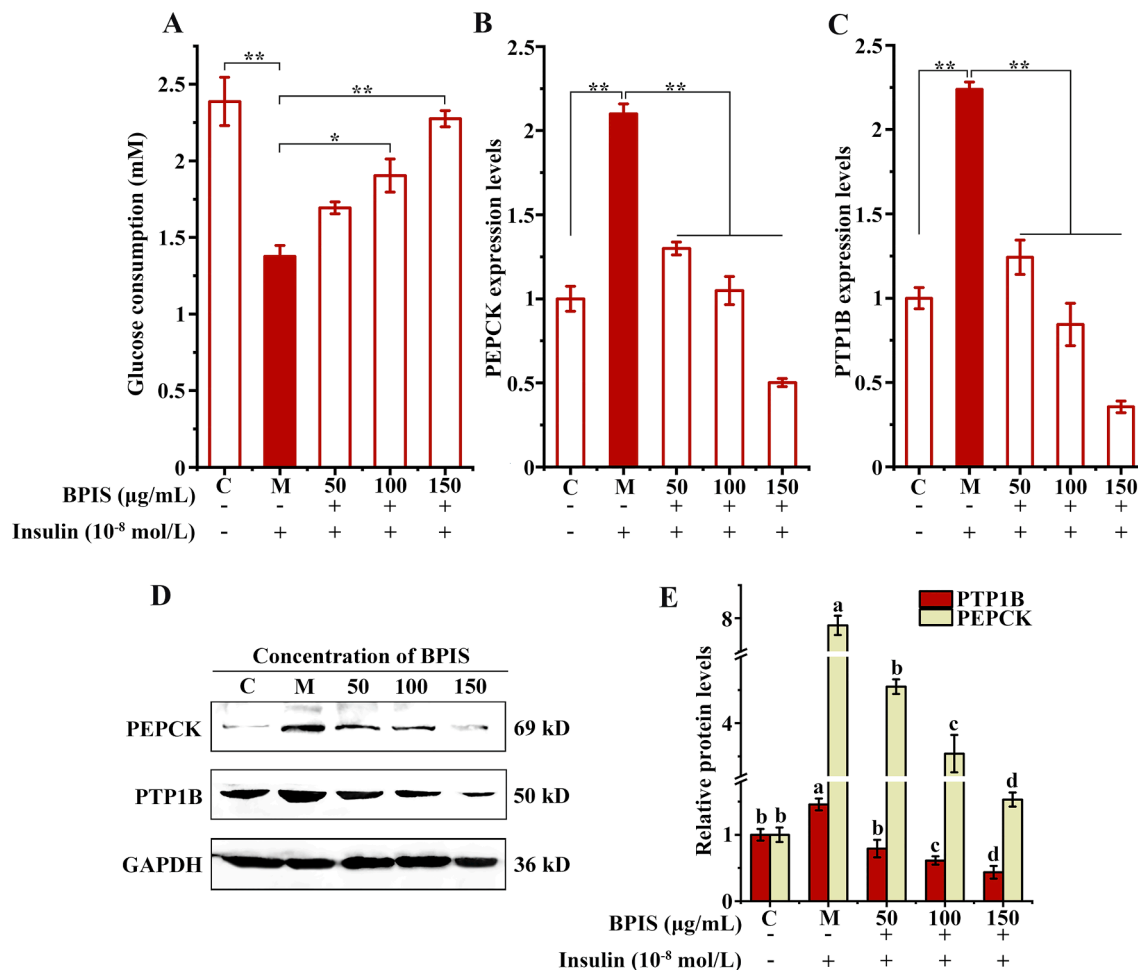


**Fig. 3.** BPIS improves insulin resistance. (A) Glucose consumption of insulin resistant HepG2 cells was measured after treatment with different doses of BPIS (50, 100, 150  $\mu$ g/mL). \* $p$  < 0.05, \*\* $p$  < 0.01. (B, C) The mRNA levels of PEPCK and PTP1B in insulin resistant HepG2 cells were detected after treatment with different doses of BPIS (50,100, 150  $\mu$ g/mL). (D) Western blot was used to detect the expression of PEPCK and PTP1B in insulin resistant HepG2 cells treated with different doses of BPIS (50, 100, 150  $\mu$ g/mL). (E) The relative protein expression levels of PEPCK and PTP1B were analyzed by Image J. The significant difference was indicated by different letters between groups, \* $p$  < 0.05.

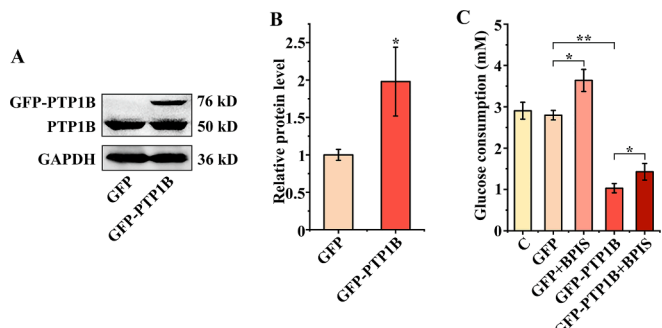


**Fig. 4.** BPIS improves insulin resistance by regulating the expression of PTP1B. (A) Western blot was used to detect the expression level of PTP1B in HepG2 cells after transfection. (B) The PTP1B expression level of protein were analyzed by Image J. (C) Effects of transfection and treated with BPIS (100  $\mu$ g/mL) on glucose consumption of HepG2 cells. All data were shown as the mean  $\pm$  SD ( $n \geq 3$ ) and analyzed by ANOVA, followed by Tukey's post-hoc test. \* $p < 0.05$ , \*\* $p < 0.01$ .

regulated more than 10 times compared with cells transfected with GFP (Fig. S4C). At the protein level, the expression of PTP1B was significantly up-regulated after transfection with GFP-PTP1B (Fig. 4A and B), further demonstrating successful overexpression of PTP1B in HepG2 cells. As shown in Fig. 4C, the comparison between the GFP + BPIS group and GFP-PTP1B + BPIS group revealed that the overexpression of PTP1B significantly reduced the glucose consumption rate of BPIS, indicating that the overexpression of PTP1B significantly reversed the remission effect of BPIS on insulin resistance. These results suggest that PTP1B plays an important role in the improvement of insulin resistance by BPIS.

### 3.5. BPIS improves insulin resistance by up-regulating miR-1-3p and inhibiting its target protein PTBP1

In order to clarify the role of miRNA in the regulation of insulin-resistant by BPIS, miRNAs bind to the 3'UTR (3'non-coding region) of PTP1B gene were predicted by three softwares: miRBase, TargetScan 7.2 and miRDB. The predicted results are shown in Fig. 5B, the 3'UTR region of the PTP1B gene has a binding site for miR-1-3p. We further explored miR-1-3p expression by BPIS treatment in the insulin-resistant HepG2 cell model. The RNA expression of miR-1-3p was significantly recalled after BPIS treatment in a dose-dependent manner (Fig. 5A). Therefore, BPIS could also significantly increase the expression of miR-1-3p in insulin-resistant HepG2 cells. Further, effects of PTP1B expression and glucose consumption in insulin-resistant HepG2 cells were analyzed by miR-1-3p inhibitor and mimic. As shown in Fig. 5C and D, miR-1-3p inhibitor down-regulated the expression of miR-1-3p, while miR-1-3p mimic up-regulated the expression of miR-1-3p, indicating that both miR-1-3p inhibitor and miR-1-3p mimic were successfully transfected into HepG2 cells. Next, qPCR and western blot assays were used to verify the transfection effects of miR-1-3p inhibitor and mimic in insulin-resistant HepG2 cells. As shown in Fig. 5E and F, miR-1-3p inhibitor caused a significant increase in the mRNA expression of PTP1B, whereas miR-1-3p mimic resulted in a significant decrease in the mRNA expression of PTP1B. At the protein level, the changes of PTP1B expression after transfection of miR-1-3p inhibitor and miR-1-3p mimic were consistent with the results of mRNA level (Fig. 5G-H). As shown in Fig. 5I, J, miR-1-3p inhibitor can significantly reduce glucose consumption of insulin-resistant HepG2 cells, while the effect of miR-1-3p mimic is opposite to that of miR-1-3p inhibitor. In order to assess whether PTP1B was the direct target of miR-1-3p, a double-luciferase report system containing 3'UTR of PTP1B was used. Luciferase activity was significantly diminished when treated with the miR-1-3p mimic while that was increased after miR-1-3p inhibitor (Fig. 5K). These results

indicate that miR-1-3p directly regulates PTBP1. In conclusion, BPIS up-regulates miR-1-3p, which results in decreased expression of PTP1B, thereby the remission of insulin resistance.

### 3.6. BPIS alleviates the STZ-induced insulin resistance in diabetes mice

To further confirm whether BPIS could improve insulin resistance *in vivo*, diabetes model in ICR mice was constructed by STZ combined with high-glucose and high-fat diet, followed by intragastric administration with BPIS (Fig. 6A). As shown in Fig. 6B, mice in both metformin (Met) and BPIS groups lost weight compared to the control group, but their weight was upregulated in the last week. As shown in Fig. 6C, the blood glucose level of mice in the control group was always maintained at a normal level, while that of mice in the model group was above 20 mmol/L, indicating that the diabetic mouse model was successfully constructed. After 6 weeks of Met and BPIS intervention, fasting blood glucose levels in the Met and BPIS groups were  $12.3 \pm 2.01$  mmol/L and  $9.4 \pm 2.15$  mmol/L, respectively. Compared with the model group, the reduction was 1.83 times and 2.39 times, respectively. The above results indicate that BPIS can effectively reduce blood glucose level and improve the diabetic disease in mice, and its hypoglycemic effect is stronger than metformin. Further, after oral glucose for 30 min, the blood glucose of all groups reached the maximum value, among which the blood glucose of Met group and BPIS group were  $18.38 \pm 0.88$  mmol/L and  $14.47 \pm 1.18$  mmol/L, respectively, while that of model group reached  $27.67 \pm 1.55$  mmol/L. After 120 min of oral glucose, blood glucose in Met group and BPIS group was still significantly lower than that in model group (Fig. 6D). OGTT results of oral glucose tolerance are shown in Fig. 6E, compared with model group, AUC of curve area in metformin group and BPIS group decreased significantly by  $40 \pm 4.63\%$  and  $53 \pm 9.22\%$  respectively. Therefore, BPIS can significantly improve the glucose tolerance of diabetic mice. In addition, the serum insulin content and glycosylated serum protein content were detected. As shown in Fig. 6F, BPIS can significantly improve insulin resistance. Glycosylated serum proteins can reflect the products of non-enzymatic glycation between different proteins in the serum and blood glucose, which can reflect the blood glucose level for nearly 2–3 weeks. As shown in Fig. 6G, compared with the model group, metformin and BPIS significantly inhibited glycosylated serum protein (GSP), which also indicates that BPIS has hypoglycemic effect. The hypoglycemic effect of BPIS was higher than that of metformin.

The liver is the main organ that regulates glycometabolism (H. R. Ding, Wang, Ren, & Shi, 2018), and the pancreas is the only organ that secretes insulin in the body (Grodsky, 1970). Therefore, we performed histopathological examinations of BPIS and Met treated mouse livers and pancreases. As shown in Fig. 6H, mild vacuolar degeneration of hepatocytes can be seen in model group. Compared with the model group, the vacuolar degeneration of hepatocytes in the Met group were reduced, but there were inflammatory cells infiltration. However, no obvious abnormality of hepatocytes was found in the BPIS group. In addition, the acinar cells of mice were closely arranged and the structure was clear in BPIS group, but the number of islets in the pancreatic tissue of mice was less in the model group. These results indicate that BPIS effectively ameliorated islet destruction by STZ, and have no effect on the liver.

Glucose transporter 2 (GLUT2) is a glucose transporter that converts glucose into glycogen in the liver, which lowers blood sugar levels (Thorens, 2015). Therefore, we detected the effect of BPIS on GLUT2 and miR-1-3p by qPCR and western blot. The results showed that BPIS could significantly reverse the low expression of GLUT2 and miR-1-3p in the model group (Fig. 6I, K and L), while the high expression of PTP1B in the model group was significantly inhibited after BPIS treatment (Fig. 6J, K and L). In addition, the immunohistochemical results were shown in Fig. 6M, PTP1B was highly expressed and GLUT2 was low expressed in the model group, and the Met group and the BPIS treatment group could reverse this phenomenon in the liver (Fig. 6N-O). These

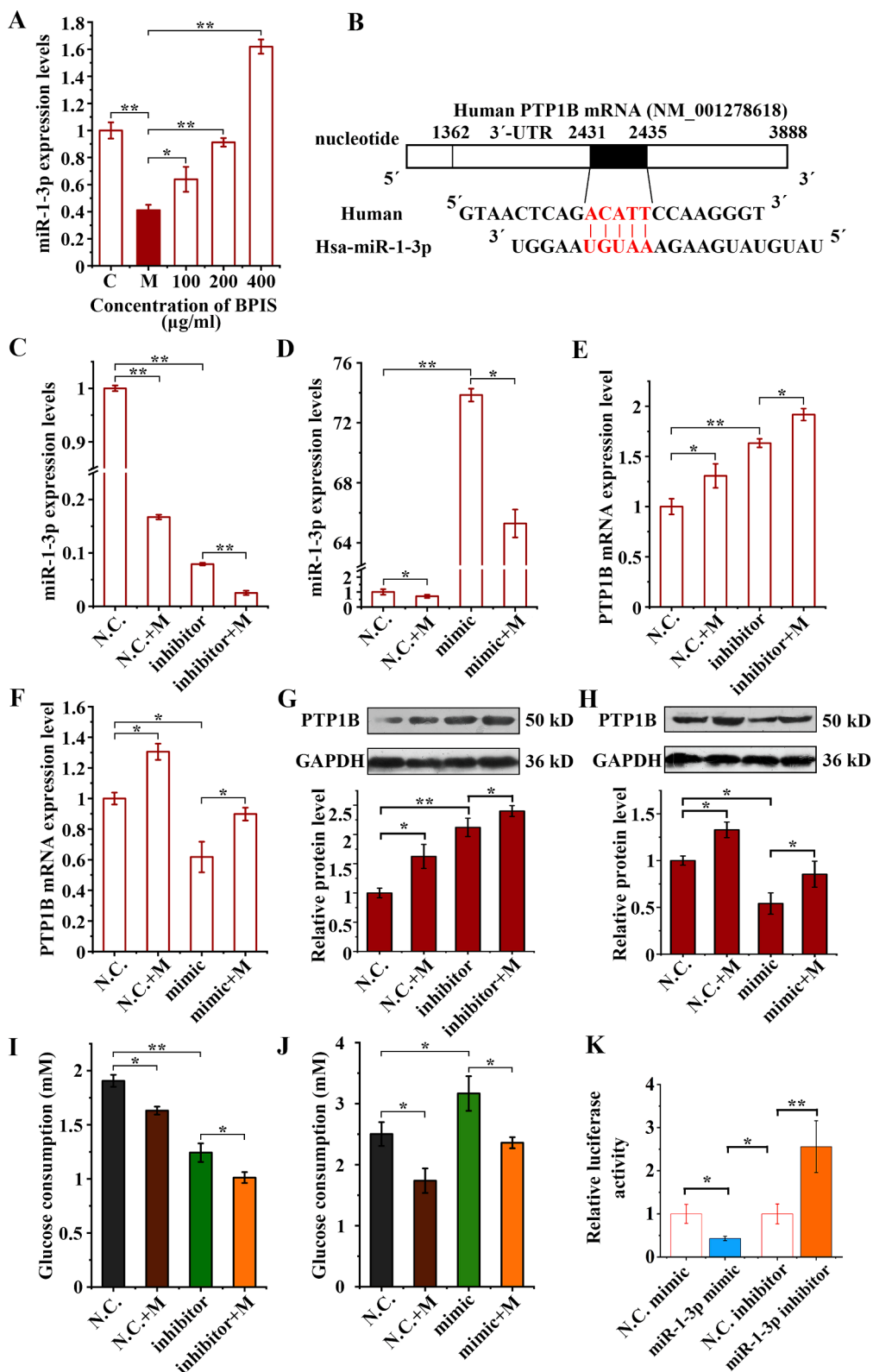


**Fig. 5.** BPIS can improve insulin resistance through miR-1-3p/PTP1B signaling pathway. (A) Changes of miR-1-3p expression in insulin resistant HepG2 cells and treated with different dosages (50, 100, 150 μg/mL) BPIS were detected by qPCR. (B) The sequences of PTP1B 3'-UTR showing complementary pairing with miR-1-3p. (C, D) The expression of miR-1-3p in HepG2 cells treated with miR-1-3p inhibitor and miR-1-3p mimic. (E, F) The mRNA expression of PTP1B in HepG2 treated with miR-1-3p inhibitor and miR-1-3p mimic. (G, H) The protein expression of PTP1B in HepG2 cells treated with miR-1-3p inhibitor and miR-1-3p mimic. The relative expression levels of protein were analyzed by Image J. (I, J) Effect of glucose consumption on HepG2 cells treated with miR-1-3p inhibitor and miR-1-3p mimic. (K) Luciferase reporter assay. We co-transfected 50 ng of psiCHECK-2-PTP1B 3'-UTR plasmid and 20 μM of miRNA-1-3p inhibitor, mimic, NC into HepG2 cells. The N.C treatment group inhibited the luciferase activity of the PTP1B 3'-UTR construct. By contrast, miRNA-1-3p inhibitor increased luciferase activity of the PTP1B 3'-UTR construct (\*  $p < 0.05$ , \*\*  $p < 0.01$ ). Each bar represents the mean  $\pm$  SEM of three independent experiments. All data were shown as the mean  $\pm$  SD ( $n \geq 3$ ) and analyzed by ANOVA, followed by Tukey's post-hoc test. \* $p < 0.05$ , \*\* $p < 0.01$ .

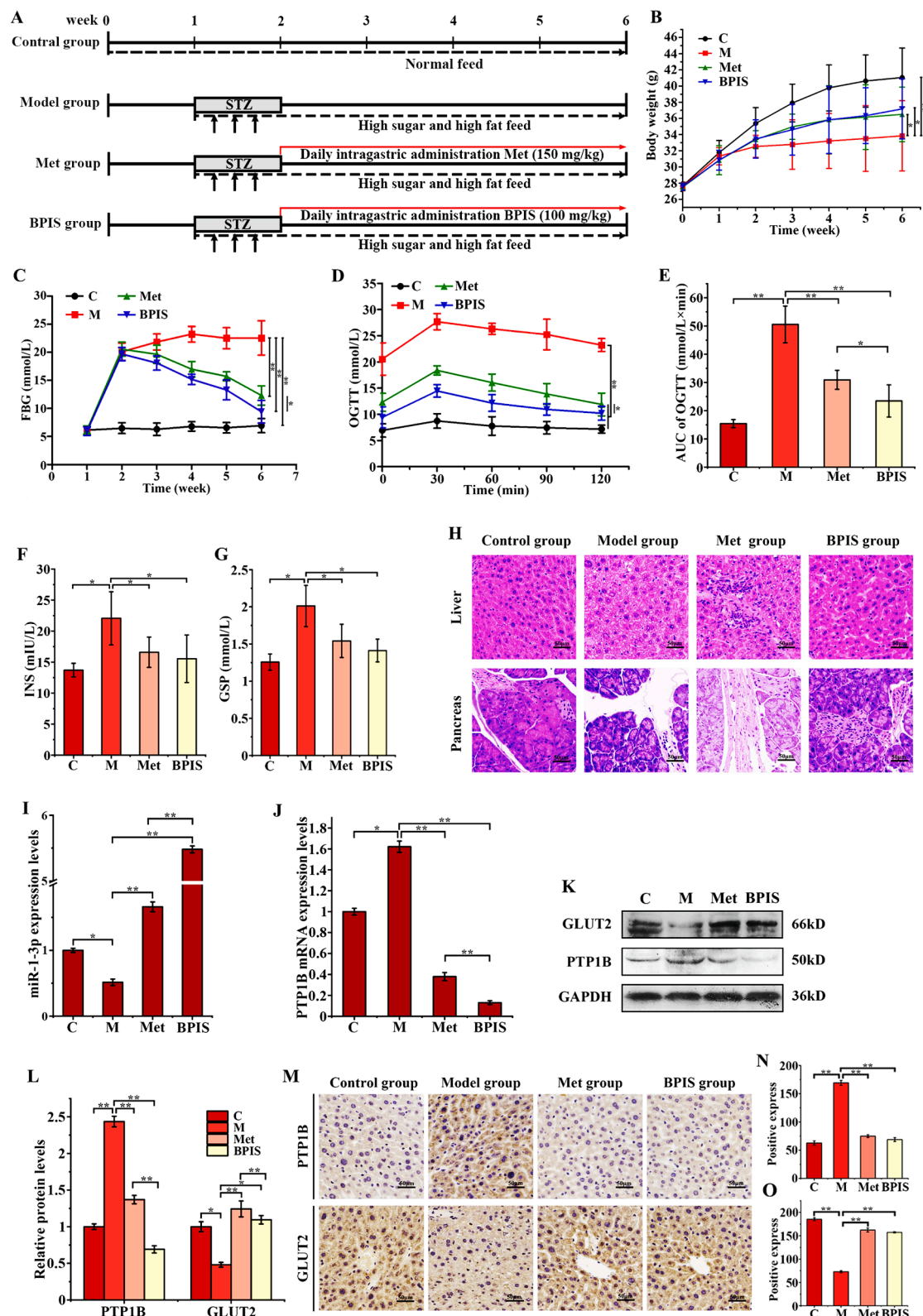


**Fig. 6.** BPIS attenuates STZ-induced insulin resistance in mice. (A) Flow chart of STZ combined with high sugar and high fat diet induced diabetic model in mice. (B) Average weight change of different group. (C) Average blood glucose value of different group. (D) Blood glucose level before and after the oral glucose tolerance test in each group was determined. (E) AUC of OGTT. Compared to model group,  $*p < 0.05$ ,  $**p < 0.01$ . C: control group; M: model group; Met: metformin group; BPIS: BPIS group. FBG: Fasting blood glucose; OGTT: Oral glucose tolerance test. (F) Changes of serum insulin in mice of different group. (G) Changes of glycosylated serum protein in different group.  $*p < 0.05$ . C: control group; M: model group; Met: metformin group; BPIS: BPIS group. (H) Effects of BPIS on main organs of STZ-induced mice by HE staining(20 $\times$ ). (I) Expression of miR-1-3p in liver of mice in each group. (J) Expression of PTP1B mRNA in liver of mice in each group. (K) Expression of glucose metabolism related proteins in liver of mice. (L) The relative expression levels of protein were analyzed by Image J.  $*p < 0.05$ ,  $**p < 0.01$ . (M) Effects of BPIS on PTP1B and GLUT2 expression in mice liver section by immunohistochemistry analysis(20 $\times$ ). (N, O) Quantitative analysis was carried out by Image J software. All data were shown as the mean  $\pm$  SD ( $n \geq 5$ ) and analyzed by Student's T-test.  $*p < 0.05$ ,  $**p < 0.01$ .

results suggest that BPIS can improve insulin resistance through the miR-1-3p/PTP1B signaling pathway in diabetic mouse model.

#### 4. Discussion

Diabetes mellitus is a chronic metabolic disease characterized by persistent hyperglycemia (Lebovitz, 2001). Alpha-glucosidase is a key enzyme that catalyzes the hydrolysis of disaccharides (maltose and sucrose) into monosaccharides (glucose and fructose). Therefore, inhibition of  $\alpha$ -glucosidase activity relieves hyperglycemia. Currently, acarbose and miglitol are approved by FDA as clinical hypoglycemic agents, both of which have the effect of inhibiting  $\alpha$ -glucosidase (Cao et al., 2019). However, these drugs cause side effects of gastrointestinal dysfunction such as stomach bloating, abdominal pain, and diarrhea, and have limiting factors that cannot be taken for a long time (Xu et al., 2018). Therefore, it is of great importance to find natural, effective and non-toxic hypoglycemic function factors. Meta-analysis studies show that polyphenols play a crucial role in the prevention of T2DM (Palma-Duran, Vlassopoulos, Lean, Govan, & Combet, 2017). Polyphenols contribute to the treatment of T2DM in various ways, such as inhibition of digestive enzymes, regulation of glucose metabolic pathways and regulation of gut microbiota (Chen et al., 2022). Based on the high content of polyphenols in plants, wide sources, large-scale synthesis, low toxicity, and the role of preventing and treating a variety of chronic diseases (Fraga, Croft, Kennedy, & Tomás-Barberán, 2019), it has become a new direction for nutritional interventions in diabetes.

Foxtail millet has gained increasing attention due to its rich nutritional value and many health benefits (L. Z. Zhang & Liu, 2015). Compared with fruits and vegetables, foxtail millet is rich in polyphenols and are mainly distributed in the foxtail millet bran (Chandrasekara & Shahidi, 2010), which have been neglected in terms of health benefits. In our previous studies, phenolic acids extracted from foxtail millet bran (BPIS) could inhibit proliferation of colon cancer cells by inhibiting glucose uptake, suggesting that BPIS may have a role in regulating glucose metabolism. Therefore, this study evaluated the effect of BPIS on  $\alpha$ -glucosidase activity by enzyme inhibitor model. The results showed that BPIS could significantly inhibit  $\alpha$ -glucosidase activity and the type of inhibition is non-competitive inhibition (Fig. 1).

Insulin resistance leads to elevated blood glucose levels, which is an important pathological feature of diabetes. Therefore, improving insulin sensitivity is the key to lowering blood glucose and alleviating diabetes. In this study, PEPCK (rate-limiting enzyme of gluconeogenic pathway) and PTP1B (negative regulator of insulin and leptin signaling) were used as key indexes to evaluate the hypoglycemic effect of BPIS. The result shows that BPIS could significantly improve the sensitivity of insulin resistance cell to insulin by reducing the expression of PEPCK and PTP1B (Fig. 3). Further, by constructing the HepG2 cell model of PTP1B over-expression, it was revealed that BPIS promoted the glucose consumption of HepG2 cells to achieve hypoglycemic activity by inhibiting the expression of PTP1B (Fig. 4). These results confirmed that PTP1B plays a key role in the improvement of insulin resistance by BPIS.

miRNAs are non-coding small RNAs with a length of nearly 21 bases, which play an important regulatory role in the life processes of living organisms (Mohr & Mott, 2015). Numerous studies have shown that certain miRNAs can trigger the pathophysiology of type II diabetes or participate in the components of the pathway, and are promising as biomarkers of T2D and its complications (Park, Jeong, Yang, & Lee, 2013). Several studies have shown that the expression of miR-24 downregulates the expression of the insulin gene transcriptional inhibitor Sox6, promoting insulin synthesis and secretion (Melkman-Zehavi et al., 2011). Arefeh et al. show that miRNAs are highly correlated with islet cell function (Jafarian et al., 2015). In order to investigate the role of miRNA in improving insulin resistance by BPIS, TargetScan 7.2 software was used to predict the complementary effect between 3-UTR of PTP1B and miR-1-3p. Some studies have shown that miR-1-3p is expressed in the peripheral blood of patients with type II diabetes mellitus

(Kokkinopoulou et al., 2019), but the molecular mechanism is not clear. In this study, the key role of the miR-1-3p/PTP1B signaling pathway in improving insulin resistance in BPIS was further demonstrated by using miR-1-3p inhibitor and mimic. Eventually, PTP1B was revealed to be a target gene for miRNA-1-3p by double lucifer reporter experiments (Fig. 5). This study demonstrated that BPIS plays an anti-diabetic role in insulin-resistant HepG2 cells by up-regulating miR-1-3p to inhibit the expression of its target gene PTP1B.

We further verified the hypoglycemic effects and safety of BPIS *in vivo*. The results showed that BPIS improved weight loss in mice with diabetes and had no side effects on the liver. The hypoglycemic effect of BPIS was higher than that of metformin. In addition, BPIS can significantly improve the glucose tolerance of mice, reduce the serum insulin content and glycoylated serum protein value of mice. Meantime, BPIS could alleviate the low expression of miR-1-3p and GLUT2, and inhibit the high expression of PTP1B in mouse liver (Fig. 6). These results suggest that miR-1-3p/PTP1B participates in STZ-induced diabetes, and BPIS can improve insulin resistance through regulating miR-1-3p/PTP1B pathway.

#### 5. Conclusion

This study investigated the effect and molecular mechanism of BPIS on improving insulin resistance *in vivo* and *in vitro*. Specifically, BPIS has a significant inhibitory effect on  $\alpha$ -glucosidase activity by the enzyme-inhibitor model test, and the inhibitory type is non-competitive inhibition. In addition, the insulin-resistant HepG2 cell model was constructed with high concentration of insulin, revealing that BPIS can significantly improve the sensitivity of the HepG2 cell model to insulin by reducing the expression of PEPCK, a key rate-limiting enzyme in gluconeogenic pathway, and PTP1B, a negative regulatory factor in insulin signaling pathway. PTP1B was further revealed as a downstream target gene of miR-1-3p at the cellular level and in mouse diabetes models. BPIS can improve insulin resistance through miR-1-3p/PTP1B signaling pathway. The findings of this study improved the development value and bioavailability of foxtail millet bran, and provided an effective experimental basis and theoretical basis for the research and development of insulin sensitizer and nutrition intervention of phenolic acids from foxtail millet bran.

#### Ethics statement

All animal protocols were reviewed and approved by the Institutional Animal Care and Use Committee of China Institute for radiation protection. Authors follow a code of ethics.

#### CRediT authorship contribution statement

**Jiangying Shi:** Writing – original draft, Funding acquisition. **Jin Wang:** Investigation, Data curation. **Shuhua Shan:** Writing – review & editing, Data curation. **Mengyun Zhao:** Data curation. **Cai Bi:** Validation. **Hanqing Li:** Writing – review & editing. **Zhuoyu Li:** Writing – review & editing, Funding acquisition.

#### Declaration of competing interest

The authors declare that they have no known competing financial interests or personal relationships that could have appeared to influence the work reported in this paper.

#### Data availability

Data will be made available on request.

## Acknowledgements

This study was supported by National Natural Science Foundation of China (No.81803238, 32072220, 32270420); National Natural Science Foundation of China Regional Innovation and Development Joint Fund Key Support Project (No.U23A20526); Shanxi Province Science Foundation (No.202203021221031, 202103021224011); The Open Project Program of Xinghuacun College of Shanxi University (Shanxi Institute of Brewing Technology) (No.XCSXU-KF-202322).

## Appendix A. Supplementary data

Supplementary data to this article can be found online at <https://doi.org/10.1016/j.jff.2024.106105>.

## References

Ali, H. S., Kamel, M. M., Agwa, S. H. A., Hakeem, M. S. A., Meteini, M. S. E., & Matboli, M. (2023). Analysis of mRNA-miRNA-lncRNA differential expression in prediabetes/type 2 diabetes mellitus patients as potential players in insulin resistance. *Front Endocrinol (Lausanne)*, 14, 1131171. <https://doi.org/10.3389/fendo.2023.1131171>

Cadoudal, T., Fouque, F., Benelli, C., & Forest, C. (2008). Glyceroneogenesis and PEPCK-C: Pharmacological targets in type 2 diabetes. *Medical Science (Paris)*, 24(4), 407–413. <https://doi.org/10.1051/medsci.2008244407>

Cao, H., Ou, J., Chen, L., Zhang, Y., Szkudelski, T., Delmas, D., & Xiao, J. (2019). Dietary polyphenols and type 2 diabetes: Human study and clinical trial. *Critical Reviews in Food Science and Nutrition*, 59(20), 3371–3379. <https://doi.org/10.1080/10408398.2018.1492900>

Chandrasekara, A., & Shahidi, F. (2010). Content of insoluble bound phenolics in millets and their contribution to antioxidant capacity. *Journal of Agricultural and Food Chemistry*, 58(11), 6706–6714. <https://doi.org/10.1021/jf100868b>

Chandrasekara, A., & Shahidi, F. (2011). Bioactivities and antiradical properties of millet grains and hulls. *Journal of Agricultural and Food Chemistry*, 59(17), 9563–9571. <https://doi.org/10.1021/jf201849d>

Chen, K., Gao, Z., Ding, Q., Tang, C., Zhang, H., Zhai, T., & Liu, W. (2022). Effect of natural polyphenols in Chinese herbal medicine on obesity and diabetes: Interactions among gut microbiota, metabolism, and immunity. *Frontiers in Nutrition*, 9, Article 962720. <https://doi.org/10.3389/fnut.2022.962720>

Ding, H. R., Wang, J. L., Ren, H. Z., & Shi, X. L. (2018). Lipometabolism and glycometabolism in liver diseases. *Biomed Research International*, 2018, 1287127. <https://doi.org/10.1155/2018/1287127>

Ding, X. Q., Gu, T. T., Wang, W., Song, L., Chen, T. Y., Xue, Q. C., & Kong, L. D. (2015). Curcumin protects against fructose-induced podocyte insulin signaling impairment through upregulation of miR-206. *Molecular Nutrition & Food Research*, 59(12), 2355–2370. <https://doi.org/10.1002/mnfr.201500370>

Fraga, C. G., Croft, K. D., Kennedy, D. O., & Tomás-Barberán, F. A. (2019). The effects of polyphenols and other bioactives on human health. *Food & Function*, 10(2), 514–528. <https://doi.org/10.1039/c8fo01997e>

Goldstein, B. J. (2001). Protein-tyrosine phosphatase 1B (PTP1B): A novel therapeutic target for type 2 diabetes mellitus, obesity and related states of insulin resistance. *Current Drug Targets. Immune, Endocrine and Metabolic Disorders*, 1(3), 265–275. <https://doi.org/10.2174/1568008013341163>

González-Rodríguez, A., Mas Gutierrez, J. A., Sanz-González, S., Ros, M., Burks, D. J., & Valverde, A. M. (2010). Inhibition of PTP1B restores IRS1-mediated hepatic insulin signaling in IRS2-deficient mice. *Diabetes*, 59(3), 588–599. <https://doi.org/10.2337/db09-0796>

Grodsky, G. M. (1970). Insulin and the pancreas. *Vitamins and Hormones*, 28, 37–101. [https://doi.org/10.1016/s0083-6729\(08\)60888-2](https://doi.org/10.1016/s0083-6729(08)60888-2)

Groop, L. (2000). Pathogenesis of type 2 diabetes: The relative contribution of insulin resistance and impaired insulin secretion. *International Journal of Clinical Practice Supplement*, (113), 3–13.

Gurnell, M., Savage, D. B., Chatterjee, V. K., & O’Rahilly, S. (2003). The metabolic syndrome: Peroxisome proliferator-activated receptor gamma and its therapeutic modulation. *The Journal of Clinical Endocrinology and Metabolism*, 88(6), 2412–2421. <https://doi.org/10.1210/jc.2003-030435>

Jafarian, A., Taghikani, M., Abroun, S., Allahverdi, A., Lamei, M., Lakpour, N., & Soleimani, M. (2015). The generation of insulin producing cells from human mesenchymal stem cells by MiR-375 and anti-MiR-9. *PLoS One*, 10(6), e0128650. <https://doi.org/10.1371/journal.pone.0128650>

Kokkinopoulou, I., Maratou, E., Mitrou, P., Boutati, E., Sideris, D. C., Fragoulis, E. G., & Christodoulou, M. I. (2019). Decreased expression of microRNAs targeting type-2 diabetes susceptibility genes in peripheral blood of patients and predisposed individuals. *Endocrine*, 66(2), 226–239. <https://doi.org/10.1007/s12020-019-02062-0>

Lebovitz, H. E. (2001). Insulin resistance: Definition and consequences. *Experimental and Clinical Endocrinology & Diabetes*, 109(Suppl 2), S135–S148. <https://doi.org/10.1055/s-2001-18576>

Liu, F., Shan, S., Li, H., Shi, J., Hao, R., Yang, R., & Li, Z. (2021). Millet shell polyphenols prevent atherosclerosis by protecting the gut barrier and remodeling the gut microbiota in ApoE(-/-) mice. *Food & Function*, 12(16), 7298–7309. <https://doi.org/10.1039/dif00991e>

Lu, Y., Shan, S., Li, H., Shi, J., Zhang, X., & Li, Z. (2018). Reversal effects of bound polyphenol from foxtail millet bran on multidrug resistance in human HCT-8/Fu colorectal cancer cell. *Journal of Agricultural and Food Chemistry*, 66(20), 5190–5199. <https://doi.org/10.1021/acs.jafc.8b01659>

McDougall, G. J., Shapiro, F., Dobson, P., Smith, P., Blake, A., & Stewart, D. (2005). Different polyphenolic components of soft fruits inhibit alpha-amylase and alpha-glucosidase. *Journal of Agricultural and Food Chemistry*, 53(7), 2760–2766. <https://doi.org/10.1021/jf0489926>

Melkman-Zehavi, T., Oren, R., Kredo-Russo, S., Shapira, T., Mandelbaum, A. D., Rivkin, N., & Hornstein, E. (2011). miRNAs control insulin content in pancreatic  $\beta$ -cells via downregulation of transcriptional repressors. *The EMBO Journal*, 30(5), 835–845. <https://doi.org/10.1038/embj.2010.361>

Mohr, A. M., & Mott, J. L. (2015). Overview of microRNA biology. *Seminars in Liver Disease*, 35(1), 3–11. <https://doi.org/10.1055/s-0034-1397344>

Palma-Duran, S. A., Vlassopoulos, A., Lean, M., Govan, L., & Combet, E. (2017). Nutritional intervention and impact of polyphenol on glycohemoglobin (HbA1c) in non-diabetic and type 2 diabetic subjects: Systematic review and meta-analysis. *Critical Reviews in Food Science and Nutrition*, 57(5), 975–986. <https://doi.org/10.1080/10408398.2014.973932>

Park, S. Y., Jeong, H. J., Yang, W. M., & Lee, W. (2013). Implications of microRNAs in the pathogenesis of diabetes. *Archives of Pharmacal Research*, 36(2), 154–166. <https://doi.org/10.1007/s12272-013-0017-6>

Ruze, R., Liu, T., Zou, X., Song, J., Chen, Y., Xu, R., & Xu, Q. (2023). Obesity and type 2 diabetes mellitus: Connections in epidemiology, pathogenesis, and treatments. *Front Endocrinol (Lausanne)*, 14, 1161521. <https://doi.org/10.3389/fendo.2023.1161521>

Samtiya, M., Aluko, R. E., Dhaka, N., Dheewa, T., & Punyi, A. K. (2023). Nutritional and health-promoting attributes of millet: Current and future perspectives. *Nutrition Reviews*, 81(6), 684–704. <https://doi.org/10.1093/nutrit/nuac081>

Shan, S., Shi, J., Li, Z., Gao, H., Shi, T., Li, Z., & Li, Z. (2015). Targeted anti-colon cancer activities of a millet bran-derived peroxidase were mediated by elevated ROS generation. *Food & Function*, 6(7), 2331–2338. <https://doi.org/10.1039/c5fo00260e>

Sireesha, Y., Kasetti, R. B., Nabi, S. A., Swapna, S., & Apparao, C. (2011). Antihyperglycemic and hypolipidemic activities of *Setaria italica* seeds in STZ diabetic rats. *Pathophysiology*, 18(2), 159–164. <https://doi.org/10.1016/j.pathophys.2010.08.003>

Thorens, B. (2015). GLUT2, glucose sensing and glucose homeostasis. *Diabetologia*, 58(2), 221–232. <https://doi.org/10.1007/s00125-014-3451-1>

Wang, H., Shen, Q., Fu, Y., Liu, Z., Wu, T., Wang, C., & Zhao, Q. (2023). Effects on diabetic mice of consuming lipid extracted from foxtail millet (*Setaria italica*): Gut microbiota analysis and serum metabolomics. *Journal of Agricultural and Food Chemistry*, 71(26), 10075–10086. <https://doi.org/10.1021/acs.jafc.3c02179>

Wang, X., He, Y., Mackowiak, B., & Gao, B. (2021). MicroRNAs as regulators, biomarkers and therapeutic targets in liver diseases. *Gut*, 70(4), 784–795. <https://doi.org/10.1136/gutjnl-2020-322526>

Wu, P., Liu, Z., Jiang, X., & Fang, H. (2020). An overview of prospective drugs for type 1 and type 2 diabetes. *Current Drug Targets*, 21(5), 445–457. <https://doi.org/10.2174/13894512066619031104653>

Xiao, T., Guo, Z., Sun, B., & Zhao, Y. (2017). Identification of anthocyanins from four kinds of berries and their inhibition activity to  $\alpha$ -glycosidase and protein tyrosine phosphatase 1B by HPLC-FT-ICR MS/MS. *Journal of Agricultural and Food Chemistry*, 65(30), 6211–6221. <https://doi.org/10.1021/acs.jafc.7b02550>

Xu, L., Li, Y., Dai, Y., & Peng, J. (2018). Natural products for the treatment of type 2 diabetes mellitus: Pharmacology and mechanisms. *Pharmacological Research*, 130, 451–465. <https://doi.org/10.1016/j.phrs.2018.01.015>

Yang, Y. M., Seo, S. Y., Kim, T. H., & Kim, S. G. (2012). Decrease of microRNA-122 causes hepatic insulin resistance by inducing protein tyrosine phosphatase 1B, which is reversed by licorice flavonoid. *Hepatology*, 56(6), 2209–2220. <https://doi.org/10.1002/hep.25912>

Zhang, L. Z., & Liu, R. H. (2015). Phenolic and carotenoid profiles and antiproliferative activity of foxtail millet. *Food Chemistry*, 174, 495–501. <https://doi.org/10.1016/j.foodchem.2014.09.089>

Zhang, Z. Y., & Lee, S. Y. (2003). PTP1B inhibitors as potential therapeutics in the treatment of type 2 diabetes and obesity. *Expert Opinion on Investigational Drugs*, 12(2), 223–233. <https://doi.org/10.1517/13543784.12.2.223>